

grated and the variation of the area during the pyrolysis process is represented in Figure 7.

According to TGA, infrared and  $^{29}\text{Si}$  MAS NMR, the gel is thermally stable up to 300 °C. The first stages of the pyrolysis process from 300 to 1000 °C correspond to the consumption of the  $\text{CH}_3$  groups and the conversion of the D units into T and then Q units. The sample can be described as a matrix of silica containing carbon, with at least some carbon atoms bound to silicon as revealed by NMR. At temperatures beyond 1300 °C, the carbothermal reduction of silica starts and silicon carbide is formed. As already noted in the literature,<sup>4</sup> the heating rate should be quite low during the pyrolysis process to prevent significant weight losses at high temperatures. A gel was pyrolyzed for 1 h at 1500 °C under an argon flow (purity: 99.999%) by using a heating rate of 2 °C/min. The starting sample was a monolithic piece of dried gel, while the pyrolyzed material appeared as a powder. An X-ray diffraction pattern obtained from this material exhibited sharp peaks corresponding to  $\beta\text{-SiC}$ .<sup>25</sup> A small amount of  $\alpha\text{-SiC}$  was also evidenced. No peaks due to  $\text{SiO}_2$  were present. If the same starting material is pyrolyzed by using argon gas with a lower purity (99.9%), the monolithic piece retains its shape but X-ray diffraction measurements reveal the presence of a mixture of crystalline  $\text{SiC}$  and  $\text{SiO}_2$  in the sample. It seems that silica has to be present in the material to obtain monolithic pyrolyzed pieces. The starting gel has an oxide-based network, and it seems that this network has to be retained to keep a monolithic piece.

(24) Inkrott, K.; Wharry, S. M.; O'Donnell, D. J. *Mater. Res. Soc. Symp. Proc.* **1986**, 73, 165.

(25) Powder Diffraction File; JCPDS 29 1129, 1979.

## Conclusion

The preparation of new precursors for the Si-C-O system using the sol-gel route has been investigated. The application of the hydrolysis-condensation process to a mixture of tetraethoxysilane and dimethyldiethoxysilane leads to the formation of monolithic pieces. A structural investigation performed by  $^{29}\text{Si}$  NMR has evidenced the formation of copolymers between the two precursors. Solid-state NMR also confirmed the presence of two kinds of units in the dried gels, D and Q units.  $^{29}\text{Si}$  MAS NMR proved to be a powerful technique for following the evolution of the local environment of the Si units during the pyrolysis process. A cleavage of the Si-C bonds and their conversion into Si-O bonds start above 300 °C. The presence of Si-C bonds in the silica network remains up to 900 °C. The material can be considered as a silicon oxycarbide glass. At 1000 °C, the transformation of Si-C bonds into Si-O bonds is completed, and the material can be described as a mixture of silica and carbon. Above 1300 °C, Si-C bonds are formed again by carbothermal reduction of the silica matrix, and at 1500 °C, crystalline silicon carbide is obtained. These copolymers between a tetraalkoxysilane and a dialkyldialkoxysilane appear to be attractive precursors for the preparation of silicon oxycarbide glasses and silicon carbide at higher temperatures. The ratio C/O can be modified according to the respective nature of the alkyl and alkoxy groups. Furthermore, monolithic pieces can be prepared that retain their shape as long as a silicon oxide or oxycarbide network is present.

**Acknowledgment.** We greatly acknowledge Jocelyne Maquet for recording the MAS NMR spectra.

**Registry No.** DEDMS, 78-62-6; TEOS, 78-10-4;  $\text{SiC}_4$ , 409-21-2.

## Solution/Gelation of Arsenic Trisulfide in Amine Solvents

Theresa A. Guiton and Carlo G. Pantano\*

Department of Materials Science and Engineering, Pennsylvania State University, University Park, Pennsylvania 16802

Received June 8, 1989

Arsenic-sulfur solutions were synthesized by dissolving amorphous arsenic trisulfide ( $\alpha\text{-As}_2\text{S}_3$ ) in anhydrous amine solvents. Ethylenediamine provided the highest solubility for  $\text{As}_2\text{S}_3$  and led to optimum gelation behavior. Thus, it was selected as the model system for this study. The emphasis of the study was the identification of the active polymerizing species in the  $\text{As}_2\text{S}_3$ -ethylenediamine solutions. The molecular transformations that occurred during the sol-to-gel and gel-to-glass transitions of fibers prepared from the  $\text{As}_2\text{S}_3$ -ethylenediamine solutions were also examined and correlated to the proposed solution species.

### Introduction

Many of the non-oxide amorphous chalcogenides are readily synthesized in bulk by melt quenching.<sup>1</sup> These glasses can then be used to fabricate bulk optics or to draw fiber-optic wave guides. In the case of thin films, vapor deposition has widely been applied.<sup>2</sup> However, the ultimate effect of such a high-temperature preparation method upon the structure, and thus properties, of the thin films cannot be ignored.<sup>3-11</sup> For example, mass spectroscopic

and Raman analyses have identified  $\text{As}_4\text{S}_6^{3-4}$  and  $\text{As}_4\text{S}_4^{5-7}$  species in the vapor phase of  $\alpha\text{-As}_2\text{S}_3$ . Furthermore, reports indicate the presence of these and other discrete molecular species in the as-deposited films.<sup>3-11</sup> Due to such inho-

(1) Hartouni, E.; Hulderman, F.; Guiton, T. *SPIE Proc.* **1984**, 505, 131-140.

(2) Keneman, S. A. *Thin Solid Films* **1974**, 21, 281-285.

(3) DeNeufville, J. P.; Moss, S. C.; Ovshinsky, S. R. *J. Non-Cryst. Solids* **1973/1974**, 13, 191-223.

(4) Lu, C. S.; Donohue, J. J. *Am. Chem. Soc.* **1944**, 66, 818.

(5) Leadbetter, A. J.; Apling, A. J.; Daniel, M. F. *J. Non-Cryst. Solids* **1976**, 21, 47.

(6) Apling, A. J.; Leadbetter, A. J.; Wright, A. C. *J. Non-Cryst. Solids* **1977**, 23, 369.

(7) Solin, S. A.; Papatheodorou, G. N. *Phys. Rev.* **1977**, B15, 2084-2090.

(8) Takahashi, T.; Harada, Y. *Solid State Commun.* **1980**, 35, 191.

(9) Zallen, R. *The Physics of Amorphous Solids*; Wiley: New York, 1983; pp 94-96.

(10) Wright, A. C.; Sinclair, R. N.; Leadbetter, A. J. *J. Non-Cryst. Solids* **1985**, 71, 295-302.

(11) Onari, S.; Asai, K.; Arai, T. *J. Non-Cryst. Solids* **1985**, 76, 243-251.

mogeneous density fluctuations, the ability to consistently fabricate homogeneous amorphous chalcogenides is extremely difficult, and not surprisingly, bulk optical properties are seldom achieved in the thin films. Thus, the potential advantages of low-temperature solution routes to amorphous chalcogenides are evident. Although the sol-gel synthesis of oxide glasses and ceramics has undergone extensive investigation during the past 20 years, minimal efforts have been extended to the non-oxide chalcogen compounds, i.e., sulfides, selenides, and tellurides.

As early as 1826,<sup>12,13</sup> Berzelius and Bineau recognized that  $\text{As}_2\text{S}_3$  was soluble in liquid ammonia. In fact, they observed that this system resulted in a gelatinous solution. For this study, then, it was assumed that organic base amines would also serve as chalcogenide solvents<sup>14</sup> and possibly lead to gelatinous systems. The solutions were synthesized by dissolution of bulk  $\alpha\text{-As}_2\text{S}_3$  in a variety of anhydrous amine solvents. The solvents included ethylenediamine, *n*-butylamine, *n*-propylamine, diethylamine, and triethylamine. These solutions were used to characterize the solution species and their associated gelation behavior. Raman and NMR spectroscopies were of primary benefit in this part of the study. The solutions were also used to draw fibers to examine the gel structure and its conversion into a dense glass through heat treatment. Other characteristics of the fibers and thin films prepared with these solutions have already been reported.<sup>15</sup> It is anticipated that once the solution species and gelation mechanism in this non-oxide, nonaqueous system are understood, it will be possible to synthesize these solutions directly by using monomeric or oligomeric precursors.

### Experimental Procedure

The desired mass of  $\alpha\text{-As}_2\text{S}_3$  glass (99.99%, General Dynamics Corp., Pomona, CA) or  $\text{c-As}_2\text{S}_3$  (natural mineral orpiment) was weighed into vacuum baked test tubes. The desired volume of anhydrous, vacuum-distilled amine was transferred into the septa-sealed test tubes containing  $\text{As}_2\text{S}_3$ . The solution concentrations ranged from 0.020 to 6.10 mol of  $\text{As}_2\text{S}_3$ /L of amine. The sealed test tubes were held within an evacuated desiccator at room temperature.

In an effort to monitor the solution rheology as a function of  $\text{As}_2\text{S}_3$  concentration, viscosity measurements were performed using the Wells-Brookfield Cone/Plate Viscometer, Model LVTD. The sample cup was maintained at 30 °C. All measurements were made at constant temperature (30 °C) as a function of shear rate.

The transitions of the amines were followed by  $^1\text{H}$  NMR spectroscopy. The  $^1\text{H}$  NMR spectra were collected on a Bruker WP 200 Fourier transform NMR spectrometer at an operating frequency of 200 MHz. Fully deuterated dimethyl sulfoxide (DMSO) with 1% tetramethylsilane (TMS) was used as the reference solvent.

Resonance Raman spectroscopic measurements were made using a Jobin Yvon D'Instruments SA Ramanor spectrometer. The monochromatic excitation source was a 15-mW Spectra-Physics He-Ne laser using an excitation wavelength of 632.8 nm with an effective power of 7 mW at the focal spot. Solution specimens were syringed into septa-sealed Pyrex sample vials. The resulting Raman spectra were measured by using a back-scattering technique and analyzed by using a double-monochromator system.

The structural changes occurring in the gel were monitored via microfocus Raman spectroscopy of the amorphous fibers generated from the  $\text{As}_2\text{S}_3$ /amine solutions. The fibers were simply pulled from the solutions by using capillary tubing within an inert-at-

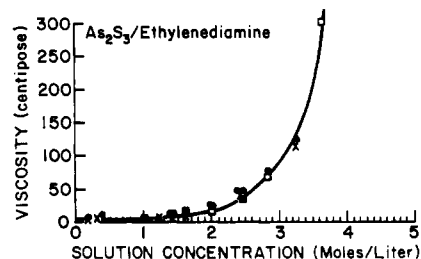


Figure 1.  $\text{As}_2\text{S}_3$ /ethylenediamine solution viscosity as a function of  $\text{As}_2\text{S}_3$  concentration.

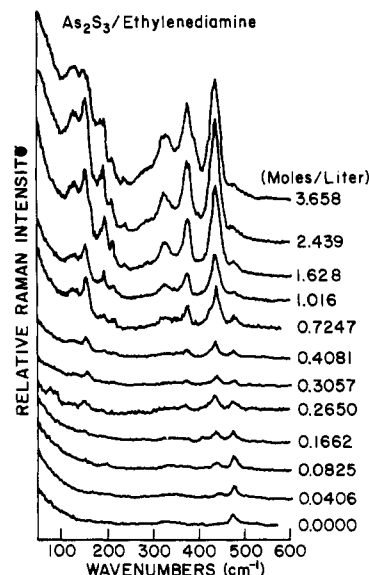


Figure 2.  $\text{As}_2\text{S}_3$ /ethylenediamine Raman spectra as a function of concentration (50–600  $\text{cm}^{-1}$ ).

mosphere glovebag. The fibers were aged in a desiccator and/or heat treated in a vacuum tube furnace ( $1.8 \times 10^{-6}$  Torr) to 180 °C. After heat treatment, the fibers were transferred to a vacuum desiccator and stored until further characterization.

### Results and Discussion

**$\text{As}_2\text{S}_3$ /Amine Solutions.** It was found that solutions of  $\text{As}_2\text{S}_3$  can be synthesized by dissolution of bulk  $\alpha\text{-As}_2\text{S}_3$  or  $\text{c-As}_2\text{S}_3$  in a variety of anhydrous amine solvents.<sup>16</sup> The solvents examined included ethylenediamine, *n*-butylamine, *n*-propylamine, diethylamine, and triethylamine. The solutions were clear and ranged in color from pale yellow to amber. The color was monitored by UV spectroscopy and was found to depend on the  $\text{As}_2\text{S}_3$  concentration. Each system also indicated a concentration-dependent increase in viscosity. Hence, the viscosity of each system was limited by its solubility of  $\text{As}_2\text{S}_3$ . Ethylenediamine provided the highest solubility for  $\text{As}_2\text{S}_3$  and led to optimum gelation behavior. Thus, it was selected as the model system for this study.

It was found that the  $\text{As}_2\text{S}_3$ /ethylenediamine solution viscosity increased with the  $\text{As}_2\text{S}_3$  concentration. This is shown quantitatively in Figure 1. At concentrations greater than 3.5 M, it was impossible to remove an adequate volume of the sample from the reaction test tube, and thus the solution viscosity measurements were not made. The measured solutions exhibited Newtonian behavior.

**Raman Spectra of Solutions.** The Raman spectra in Figure 2 were collected as a function of  $\text{As}_2\text{S}_3$  concentra-

(12) Berzelius, J. J. *Ann. Chim. Phys.* 1826, 32, 166.

(13) Bineau, A. *Ann. Chim. Phys.* 1839, 70, 54.

(14) Chern, G. C.; Lauks, I. J. *Appl. Phys.* 1982, 53(10), 6979–6982.

(15) Guiton, T. A.; Pantano, C. G. *Mater. Res. Soc. Symp. Proc.* 1988, 121, 509–514.

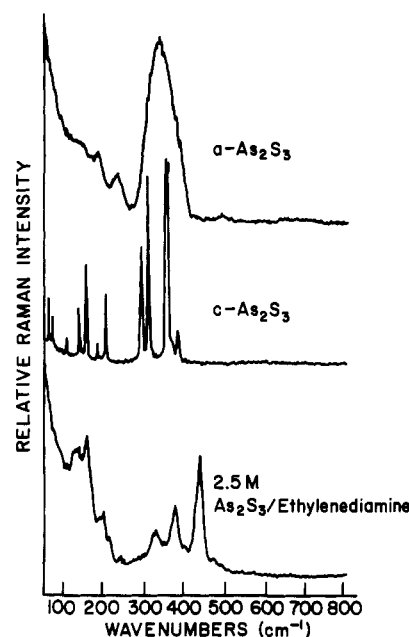
(16) Guiton, T. A. M.S. Thesis, Pennsylvania State University, Aug 1987.

**Table I. Raman Assignments of  $\alpha$ -As<sub>2</sub>S<sub>3</sub>,  $\alpha$ -As<sub>4</sub>S<sub>4</sub>,  $\beta$ -As<sub>4</sub>S<sub>4</sub>, c-As<sub>2</sub>S<sub>3</sub>, a-As<sub>2</sub>S<sub>3</sub>, and As<sub>2</sub>S<sub>3</sub>/Ethylenediamine (80–600 cm<sup>-1</sup>)**

obsd freq				predicted freq a-As <sub>2</sub> S <sub>3</sub> [26]	obsd freq a-As <sub>2</sub> S <sub>3</sub>	obsd soln freq
a-As <sub>2</sub> S <sub>3</sub> [22]	$\alpha$ -As <sub>2</sub> S <sub>3</sub> [23]	$\beta$ -As <sub>4</sub> S <sub>4</sub> [23]	c-As <sub>2</sub> S <sub>3</sub> [24]			
117		118		106		
	123					124
134			136	133		130–132
143	142	143	144			
151	155	157	154, 157			154
163	165	163		162		
	171		179			
184	182	185			185	184–187
	192		203			194–196
	209–211	210				
217		215		218		214
	220–222					
		226				
231		235			234	240
			290			
			294			
			300			
308			309	310		
			312			
			324			
	328					328
341	343	342		344	340	342
350	354	351	354, 356			
360	361	360				
	368	368	368			
	374	374				374
378						378
		384	383			
				438		438

tion. In general, the solution spectra are representative of an amorphous system; that is, due to the lack of long-range order, the low-lying frequency modes (<80 cm<sup>-1</sup>) corresponding to intermolecular interactions coalesce into a broad scattering tail. This is analogous to the spectra for the a-As<sub>2</sub>S<sub>3</sub> glass shown in Figure 3. Thus, it is emphasized that the solution species are molecular, and unlike periodic crystalline modes which generate sharp peaks, the molecular modes generate broad average peaks. Both a-As<sub>2</sub>S<sub>3</sub> and c-As<sub>2</sub>S<sub>3</sub> were used to form these solutions and were found to generate equivalent Raman spectra (and <sup>1</sup>H NMR spectra). This is not surprising and simply verifies that the chemical short-range order and the intramolecular intermediate-range order of the solutions are independent of the precursor; that is, in this case, they are true solutions.

It was found advantageous to compare the solution spectra to the solid-state crystalline and amorphous arsenic sulfide vibrational modes. These materials have been extensively investigated, and a vast data base exists for the interpretation of spectra.<sup>17–31</sup> Table I summarizes the

**Figure 3.** Raman spectra: A, a-As<sub>2</sub>S<sub>3</sub>; B, c-As<sub>2</sub>S<sub>3</sub>; C, 2.5 M As<sub>2</sub>S<sub>3</sub>/ethylenediamine.

corresponding frequency assignments. The striking feature of the crystalline spectrum in Figure 3 is the clear division of three separate frequency regions. The intramolecular modes are confined to frequencies less than 80 cm<sup>-1</sup>. The bond bending modes are centered from 120 to 225 cm<sup>-1</sup>,

- (17) Zallen, R.; Slade, M. L. *Phys. Rev. B* **1978**, *18*(10), 5775–5798.  
 (18) Zallen, R.; Slade, M. L.; Ward, A. T. *Phys. Rev. B* **1971**, *3*, 4257–4273.  
 (19) Ward, A. T.; Myers, M. B. *J. Phys. Chem.* **1969**, *73*, 1374–1380.  
 (20) Forneris, R. *Am. Mineral.* **1969**, *54*, 1062–1074.  
 (21) Wood, E. A. *Bell Syst. Tech. J.* **1964**, *43*, 541.  
 (22) Bertoluzza, A.; Fagnano, C.; Monti, P.; Semeraro, G. *J. Non-Cryst. Solids* **1978**, *29*, 49–60.  
 (23) Slade, M. L.; Zallen, R. *Solid State Commun.* **1979**, *30*(6), 357–360.  
 (24) Kobliska, R. J.; Solin, S. A. *Phys. Rev. B* **1973**, *8*(2), 756–768.  
 (25) Kobliska, R. J.; Solin, S. A. *Solid State Commun.* **1982**, *10*, 231–234.  
 (26) Lucovsky, G.; Martin, R. M. *J. Non-Cryst. Solids* **1972**, *8*(10), 185–190.  
 (27) Bermudez, V. *J. Chem. Phys.* **1972**, *57*, 2793.  
 (28) Taylor, P. C.; Bishop, S. G.; Mitchell, D. L. *Phys. Rev. Lett.* **1971**, *27*, 414.

- (29) Vaipolin, A. A.; Porai-Koshits, C. A. *Fiz. Tverd. Tela (Sov. Phys. Solid State)* **1963**, *5*, 479.  
 (30) Nemilov, S. V. *Fiz. Tverd. Tela (Sov. Phys. Solid State)* **1964**, *6*, 1075.  
 (31) Busse, L. E.; Nagel, S. R. *Phys. Rev. Lett.* **1981**, *47*, 1848.

Table II.  $^1\text{H}$  NMR Chemical Shifts as a Function of  $\text{As}_2\text{S}_3$ /Ethylenediamine Concentration

solute	amine				concn, mol/L	a	b	c	d
	a	b	c	d					
a- $\text{As}_2\text{S}_3$	$\text{NH}_2\text{-CH}_2\text{-CH}_2\text{-NH}_2$				0.0305	1.15	2.28	2.28	1.15
a- $\text{As}_2\text{S}_3$	$\text{NH}_2\text{-CH}_2\text{-CH}_2\text{-NH}_2$				0.0305	1.19	2.28	2.28	1.19
a- $\text{As}_2\text{S}_3$	$\text{NH}_2\text{-CH}_2\text{-CH}_2\text{-NH}_2 + \text{H}_2\text{O}$				0.0305	1.98	2.28	2.28	1.98
c- $\text{As}_2\text{S}_3$	$\text{NH}_2\text{-CH}_2\text{-CH}_2\text{-NH}_2$				0.0303	1.19	2.28	2.28	1.19
a- $\text{As}_2\text{S}_3$	$\text{NH}_2\text{-CH}_2\text{-CH}_2\text{-NH}_2$				3.25	2.14	2.34	2.34	2.14
a- $\text{As}_2\text{S}_3$	$\text{NH}_2\text{-CH}_2\text{-CH}_2\text{-NH}_2$				3.66	2.16	2.35	2.35	2.16
a- $\text{As}_2\text{S}_3$	$\text{NH}_2\text{-CH}_2\text{-CH}_2\text{-NH}_2$				4.06	2.36	2.36	2.36	2.36
a- $\text{As}_2\text{S}_3$	$\text{NH}_2\text{-CH}_2\text{-CH}_2\text{-NH}_2$				6.09	2.95	2.40	2.40	2.95

while the bond stretching vibrations are centered from 390 to  $385\text{ cm}^{-1}$ . In contrast, the dominant feature in the amorphous  $\text{As}_2\text{S}_3$  Raman spectrum is a broad band centered about  $340\text{ cm}^{-1}$ , the dominant stretching frequency region of crystalline  $\text{As}_2\text{S}_3$ .

To explain the vibrational spectra of a- $\text{As}_2\text{S}_3$ , two structural models have been formulated: (1) the molecular model,<sup>26</sup> associating the observed vibrational bands with the intramolecular and intermolecular vibrations of the  $\text{AsS}_3$  pyramidal structural unit, and (2) the planar random network model,<sup>27</sup> associating the observed vibrational bands with the Gaussian distribution of As-S-As bond angles while the S-As-S bond angle is fixed at  $120^\circ\text{C}$ . Raman and infrared spectra and the calculated densities of vibrational states of a- $\text{As}_2\text{S}_3$  are in agreement with both structural models. However, Kobliska and Solin<sup>24</sup> found that only the molecular model is compatible with the depolarization spectrum of a- $\text{As}_2\text{S}_3$ .

Clearly, the solution spectra do not distinctly resemble either the a- $\text{As}_2\text{S}_3$  or c- $\text{As}_2\text{S}_3$  Raman spectra; this comparison is shown in Figure 3. The biggest difference is the creation of a new band centered at about  $438\text{ cm}^{-1}$ . In Lucovsky's proposed molecular model for a- $\text{As}_2\text{S}_3$ ,<sup>26</sup> he calculates predicted vibrational modes corresponding to As-S-As "water-like" molecules. Although it was never observed for a- $\text{As}_2\text{S}_3$ , his calculations predict a weak asymmetric As-S-As stretch at  $438\text{ cm}^{-1}$ . Thus, the  $438\text{-cm}^{-1}$  mode may involve As-S-As vibrations; however, because the mode is very strong, another assignment is more probable. Raman spectra of sulfur dissolved in ethylenediamine indicate a strong  $438\text{-cm}^{-1}$  peak.<sup>32</sup> The band was attributed to a sulfur-sulfur stretching mode and will be so assigned for the  $\text{As}_2\text{S}_3$ /ethylenediamine system. Otherwise, with the exception of the pyramidal  $\text{AsS}_3$  bending mode at  $133$  and  $154\text{ cm}^{-1}$ , the remaining modes in the solution spectra correspond to the  $\text{As}_4\text{S}_4$  resonances,  $124$ ,  $184$ ,  $187$ ,  $196$ ,  $214$ , and  $240\text{ cm}^{-1}$ . Within the As-S stretching region—unlike the broad band centered at  $340\text{ cm}^{-1}$  for a- $\text{As}_2\text{S}_3$  glass—the solutions exhibit two distinct stretching modes centered at  $328$  and  $376\text{ cm}^{-1}$ . Neither mode is active in  $\text{As}_2\text{S}_3$ ; however, both are active in  $\text{As}_4\text{S}_4$ . This observation provides further evidence in favor of  $\text{As}_4\text{S}_4$  type species.

**$^1\text{H}$  NMR Spectra of Solutions.** The primary reason for examining the  $^1\text{H}$  NMR spectra of the  $\text{As}_2\text{S}_3$ /ethylenediamine solutions was to determine if amine salts or sulfur hydride species were present. Again, the series of solutions with variable  $\text{As}_2\text{S}_3$  concentration were examined. Table II lists the corresponding chemical shifts. When  $0.0305\text{ M}$  a- $\text{As}_2\text{S}_3$ /ethylenediamine was examined, the chemical shifts were  $\delta$  1.19 and 2.28; thus, the N-H amine shift is moving downfield while the C-H shift remains constant. When  $0.0303\text{ M}$  c- $\text{As}_2\text{S}_3$ /ethylenediamine was examined, the chemical shifts were once again  $\delta$  1.19 and 2.28. Hence, neither solutions exhibited the shift

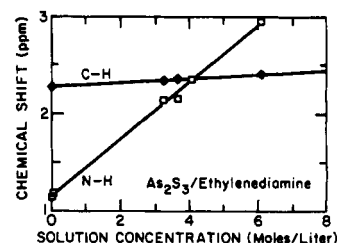


Figure 4.  $^1\text{H}$  NMR chemical shift as a function of  $\text{As}_2\text{S}_3$ /ethylenediamine solution concentration: A, N-H chemical shift; B, aliphatic chemical shift.

corresponding to the amine salt or the downfield shift in the  $\alpha$ -protons. Thus, it was concluded that amine salt species were not present. It was also evident that the  $^1\text{H}$  NMR spectra were, in general, insensitive to the  $\text{As}_2\text{S}_3$  precursor.

As a point of interest, hydrous ethylenediamine resulted in solution oxidation and thus a shift in As/S stoichiometry. The  $^1\text{H}$  NMR spectra of a  $0.0305\text{ M}$  anhydrous solution and a  $0.0305\text{ M}$  hydrous solution were collected and compared. Both solutions exhibited the aliphatic shift at  $\delta$  2.28, indicating no interaction with the protons of water, but the hydrous solution resulted in a broad-band chemical shift centered at  $\delta$  1.98 due to N-H proton exchange with  $\text{H}_2\text{O}$ . Thus,  $^1\text{H}$  NMR served as an excellent means of indicating the presence of water and potential source of solution nonstoichiometry between arsenic and sulfur.

Because the high-viscosity solutions were of particular interest, a number of solutions of higher concentration were examined (see also Table II). Again, no amine salts were identified. However, both of the sharp singlets of ethylenediamine progressively shift downfield. Indeed, these shifts can be plotted as a linear function of  $\text{As}_2\text{S}_3$  concentration, as shown in Figure 4. This provides direct evidence for an interaction between the soluble arsenic-sulfur species and the amine solvent. Because the N-H chemical shift did not split, it can be concluded that both lone pairs of electrons of ethylenediamine are being donated, and thus ethylenediamine is behaving as a bichelating ligand. Although  $\text{PX}_3$ ,  $\text{AsX}_3$ , and  $\text{SbX}_3$ , like  $\text{NX}_3$  compounds, behave as donors owing to the presence of lone pairs, there is a major difference. Because d-orbitals are not accessible, the nitrogen atom can have no function other than simple donation; whereas, due to possessing empty d-orbitals of fairly low energy, phosphorus, arsenic, and antimony can behave as electron acceptors (Lewis acids).<sup>33</sup> Although sulfur also possesses empty d-orbitals, from an electronegativity argument the nitrogen lone pair is most likely to interact with arsenic  $\delta^+$  species rather than sulfur  $\delta^-$  species. Thus, it is proposed that ethylenediamine is chelating between two arsenic centers via the donation of lone pairs of electrons; this model is shown schematically

(32) Daly, F. P.; Brown, C. W. *J. Phys. Chem.* 1973, 77, 1859-1861.

(33) Cotton, F. A.; Wilkinson, G. *Advanced Inorganic Chemistry*; Wiley: New York, 1980; p 440.

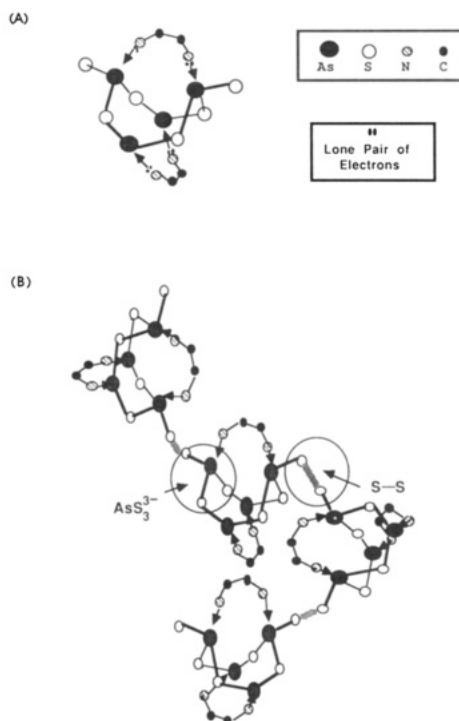


**Figure 5.** Proposed  $\text{As}_2\text{S}_3$ /ethylenediamine solution species: A, Lewis acid-base chelation model ( $\text{As}_4\text{S}_6 + \text{H}_2\text{NCH}_2\text{CH}_2\text{NH}_2$ ); B, branched chains.

in Figure 5A. Due to the Lewis acid-base interaction,  $\text{H}^{\delta+}-\text{N}^{\delta-} \rightarrow \text{As}^{\delta+}$ , the electron density about nitrogen will decrease, thus contributing to the downfield shift. The chemical shift dependence on  $\text{As}_2\text{S}_3$  concentration is attributed to hydrogen bonding and exchange. The aliphatic shift is probably due to the chelating effect, which results in a geometrical redistribution of orbital interactions and hence electron density.

**Raman Spectra of Gels.** The Raman spectra of the viscous solutions were examined after 24 h, 1 week, and 1 month time periods. During this time, a progressive increase in the solution viscosity was observed. Although a minor decrease in the  $438\text{-cm}^{-1}$  mode was observed after 1 month, the change was within the experimental error of measurement. In general, Raman spectroscopy of amorphous systems is sensitive to molecular symmetry and not intermolecular interactions. Thus, if one assumes that increases in the solution viscosity are due to intermolecular interactions, this result is not surprising. Perhaps it is surprising, though, that the fibers that were drawn from the viscous solutions and aged in a desiccator also exhibited Raman spectra comparable to those of the solutions. This comparison is shown in the lower two spectra of Figure 6. The relative intensity between the  $438\text{-cm}^{-1}$  and the  $378\text{-cm}^{-1}$  modes is reduced by 20% in the gel fiber. This result indicates that rearrangement and/or polymerization of the gel may be occurring during aging and drying of the gel. Altogether, though, the Raman spectra indicate that the extent of solution reaction or polymerization is minimal upon gelation and drying. This is very different from the situation for a silicate gel where drying of the gel can create a large number of new Si-O-Si linkages in the structure.

On the other hand, dramatic changes were observed in the Raman spectra of the gels after they were heat treated in vacuum (see also Figure 6). A number of critical results are evident. First, the  $476\text{-cm}^{-1}$  vibrational mode associated with the backbone deformation of the ethylenediamine solvent is eliminated with heat treatment. Infrared analysis also confirmed the loss of the occluded amine

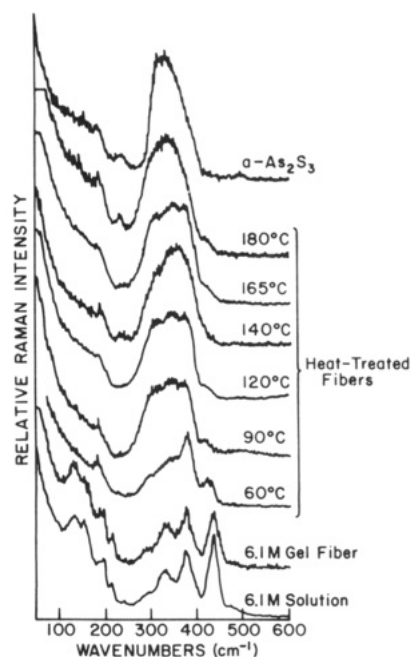


**Figure 6.** Raman spectra ( $50\text{--}600\text{ cm}^{-1}$ ): A,  $6.1\text{ M As}_2\text{S}_3$ /ethylenediamine solution; B,  $6.1\text{ M}$  gelled fiber; C-H, thermally treated gel fibers; I, reference  $\alpha\text{-As}_2\text{S}_3$ .

solvent. Second, the distinct bending modes of the solution ( $133$ ,  $154$ ,  $214$ , and  $240\text{ cm}^{-1}$ ) are smeared under the scattering tail in the heat-treated solids. Furthermore, at temperatures in excess of  $140^\circ\text{C}$ , the bending modes correspond to  $\alpha\text{-As}_2\text{S}_3$  glass. But the most dramatic effects occur in the fundamental As-S stretching region,  $440\text{--}240\text{ cm}^{-1}$ . The primary result of the heat treatment is the loss of the intense  $438\text{-cm}^{-1}$  mode associated with  $=\text{As}-\text{S}-\text{S}-\text{As}=\text{ resonances}$ .

The  $60^\circ\text{C}$  thermally treated sample provides further insight about the polymerization process. The distinct solution modes at  $298$ ,  $332$ , and  $378\text{ cm}^{-1}$  begin to overlap and coalesce into a "three-mode" broad band within the amorphous  $\text{As}_2\text{S}_3$  stretching region. In addition, associated with the loss of the  $438\text{-cm}^{-1}$  mode is the creation of a weak  $415\text{-cm}^{-1}$  side mode. As the heat-treatment temperature is increased from  $60$  to  $180^\circ\text{C}$ , the line broadening within the As-S stretching region shifts toward lower frequencies and is centered at about  $340\text{ cm}^{-1}$ . Upon transcending the glass transition temperature of  $\text{As}_2\text{S}_3$ , the band shape in the As-S stretching region resembles that of  $\alpha\text{-As}_2\text{S}_3$  glass (see Figure 6). (Note: TEM analysis of the gel heat treated to  $180^\circ\text{C}$  verified that it was fully dense.)

**Structural Model of  $\text{As}_2\text{S}_3$ /Ethylenediamine Solutions and Gels.** Unlike the structurally distinct crystalline and amorphous  $\text{As}_2\text{S}_3$  solutes, the equilibrium solutions obtained via dissolution of these solutes in amine solvents are chemically and structurally equivalent. The resulting Raman spectra of the solutions reveal  $\text{As}_4\text{S}_6$ ,  $\text{AsS}_3$ , and S-S. The spectroscopic analysis revealed no amine salts, sulfur hydride, or sulfur nitride species. These observations support the model of nitrogen behaving as a Lewis base, donating its lone pair of electrons to the empty d-orbitals of arsenic. Due to the bidentate nature of ethylenediamine, it is most likely chelating two arsenic centers,  $-\text{As}:\text{NH}_2-\text{CH}_2-\text{CH}_2-\text{H}_2\text{N}:\text{As}-$  (see Figure 5A). If indeed ethylenediamine chelates two arsenic centers, the two arsenic species will be drawn closer together, and the  $\text{As}_4\text{S}_6$  nature of the molecular unit will become vibrationally distinct.

Because the spectra do not distinctly resemble the molecular layer vibrational modes of crystalline  $\text{As}_2\text{S}_3$  and because the probability of ethylenediamine bichelating



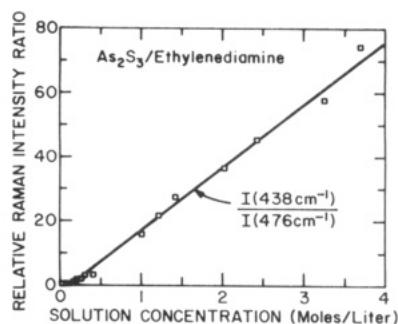


**Figure 7.** Relative Raman peak intensity ( $I_{438\text{ cm}^{-1}}/I_{476\text{ cm}^{-1}}$ ) as a function of  $\text{As}_2\text{S}_3$ /ethylenediamine solution concentration.

between crystalline layers is lower than within layers, it is concluded that the resulting soluble species are composed of As-S rings interlinked through bridging sulfurs. The resulting species resemble branched  $\text{As}_4\text{S}_6$  chains (see Figure 5B). The structure of the amorphous  $\text{As}_2\text{S}_3$  solute resemble a molecular ring network. Apparently, the solubility effect of ethylenediamine is due to a weakening of the dimensionality of the  $\text{As}_2\text{S}_3$  ring network.

These conclusions are supported by similar chemistry reported by Porter and Sheldrick.<sup>34,35</sup> They identified  $[\text{As}_4\text{S}_6]^{2-}$  via x-ray crystal identification of the salt  $[\text{C}_5\text{H}_{12}\text{N}]^+_2[\text{As}_4\text{S}_6]^{2-}$  formed by the action of piperidine ( $\text{C}_5\text{H}_9\text{N}$ ) on a solution of  $\text{As}_4\text{S}_6$  in  $\text{CH}_3\text{NH}[\text{CH}_2]_2\text{OH}$ . But, their system contained a proton source, and amine salts were generated. In contrast, the  $\text{As}_2\text{S}_3$ /anhydrous ethylenediamine solutions currently under investigation do not possess an available proton source; thus, the examined solutions do not yield salts. The postulation that a similar species,  $\text{As}_4\text{S}_6$ , exists in the ethylenediamine solution is not unreasonable. Here, the units are not distinct ions; rather, they are linked through terminal sulfurs.

The intense  $438\text{-cm}^{-1}$  solution mode, which is attributed to  $=\text{As}-\text{S}-\text{S}-\text{As}=$  stretching resonances between discrete  $\text{As}_4\text{S}_6$  species, increased linearly with increasing  $\text{As}_2\text{S}_3$  concentration (see Figure 7). It is not observed in  $\text{As}_2\text{S}_3$  glass; hence, it is a measure of the connectivity and homogeneity of the gel-derived  $\text{As}_2\text{S}_3$  network.

During the gel thermal treatment, one can envision a number of simultaneous processes occurring to the gel (Figure 8A). First, the loss of occluded amine will lead to reduced As-As orbital overlap (Figure 8B). In turn, this will enhance the stability of  $\text{AsS}_3$ , leading to the elimination of  $=\text{As}-\text{S}-\text{S}-\text{As}=$  features (Figure 8C). The details of this process are not completely clear but certainly correspond to polymerization of the molecular gel into a dense amorphous solid (Figure 8D).

This structural model is consistent with the physical behavior and characteristics of the solutions. It is believed that the viscosity behavior of the solutions is a direct result of chain entanglements. As the  $\text{As}_2\text{S}_3$  concentration increases, the viscosity increases due to a number of factors, including increasing chain concentration, length, and branching. The model is also consistent with the physical behavior of the resulting  $\text{As}_2\text{S}_3$  solids. Transmission electron microscopy confirmed that the thermally treated fibers were homogeneous, and not phase-separated, amorphous solids.

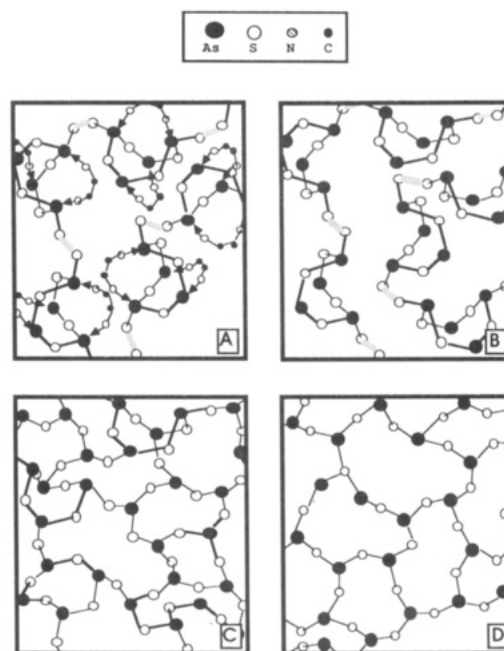
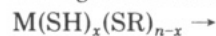


**Figure 8.** Proposed  $\text{As}_2\text{S}_3$ /ethylenediamine gel-to-glass transitions: A, solution species; B, amine loss; C, elimination of As-S-S-As; d, amorphous network.

### Conclusions

This study was initiated to uncover any generic aspects of the solution/gelation behavior of sulfide compounds. It was hypothesized that soluble sulfide species—in protonated solvents—might condense to form inorganic network gels in a manner analogous to oxide gels, e.g.



$$\text{MS}_{n/2} + (n-x)\text{RSH} + \left(\frac{2x-n}{2}\right)\text{H}_2\text{S}$$

However, it has been found that the solutions and gels, in the arsenic sulfide system at least, are molecular in nature. The soluble species are molecular complexes and chelates of the solvent. The solution viscosity depends upon the solute concentration and not necessarily upon the extent of any condensation reactions. So too, the gelation behavior is due to the concentration effects of solvent extraction. In this sense, they are more analogous to true polymer solutions than the oxide sol/gel systems, and in practice, their viscosity characteristics may be more amenable to rheological processing. Nevertheless, it must be emphasized that the soluble molecular complexes observed in the arsenic-sulfur system may be unique due to the empty d-orbitals of arsenic and their interaction with the nitrogen lone-pair electrons of the amine solvent. Some recent studies<sup>36,37</sup> of the solution/gelation behavior of zinc sulfide—in a wide range of solvents—seems to verify this contention. It remains to be shown whether or not a generic approach to the chemical processing of sulfides—analogue to the alkoxide processing of oxides—does indeed exist.

**Acknowledgment.** This work was supported in part by a Corning Fellowship and the Office of Naval Research Contract N0014-86-K-0191.

(34) Porter, E. J.; Sheldrick, G. M. *J. Am. Chem. Soc.* **1972**, 1347-1349.

(35) Lauer, V. W.; Becke-Goehring, M.; Sommer, K. *Z. Anorg. Allg. Chem.* **1969**, 371, 193.

(36) Guiton, T. A.; Czekaj, C. L.; Rau, M. S.; Geoffroy, G. L.; Pantano, C. G. *Mater. Res. Soc. Symp. Proc.* **1988**, 121, 503-508.

(37) Guiton, T. A.; Pantano, C. G.; Czekaj, C. L. *J. Non-Cryst. Solids*, in press.